CHEMISTRY OF MATERIALS

Article

pubs.acs.org/cm

# Influence of Defects and Synthesis Conditions on the Photovoltaic Performance of Perovskite Semiconductor $CsSnI_3$

Peng Xu,[†] Shiyou Chen,*[,‡] Hong-Jun Xiang,[†] Xin-Gao Gong,*[,†] and Su-Huai Wei*[,§]

[†]Key Laboratory for Computational Physical Sciences (Ministry of Education), State Key Laboratory of Surface Physics, and Department of Physics, Fudan University, Shanghai 200433, People's Republic of China

[‡]Key Laboratory of Polar Materials and Devices (Ministry of Education), East China Normal University, Shanghai 200241, People's Republic of China

[§]National Renewable Energy Laboratory (NREL), Golden, Colorado 80401, United States

Supporting Information

**ABSTRACT:** $CsSnI_3$ is a prototype inorganic halide perovskite that has recently been proposed as a strong candidate for photovoltaic applications because of its unique semiconductor properties. Through first-principle calculations, we show that the concentration control of intrinsic defects is critical for optimizing the photovoltaic properties of $CsSnI_3$. Under a Sn-poor condition, a high concentration of acceptor defects, such as Sn or Cs vacancies, can form easily and produce a high p-type conductivity and deep-level defects that can become electron−hole recombination centers, all with high energy. This condition is optimal for growing $CsSnI_3$ as hole-transport material in solar cells. In contrast, when Sn becomes richer, the concentration of acceptor defects decreases; therefore, the p-type conductivity may drop to a moderate level, which can increase the shunt resistance and, thus, the efficiency of the solar cells with $CsSnI_3$ as the light absorber material (LAM). However, under the Sn-rich condition, the concentration of a deep-level donor defect $Sn_I$ will increase, causing electron traping and non-radiative electron−hole recombination. Therefore, we propose that a moderately Sn-rich condition is optimal when $CsSnI_3$ is used as the LAM. The defect properties of $CsSnI_3$ are general, and the underlying chemistry is expected to be applicable to other halide perovskite semiconductors.

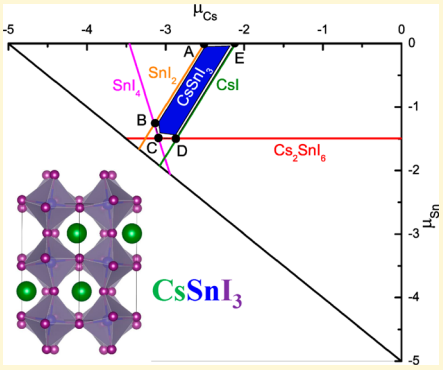


## 1. INTRODUCTION

Organometal halide perovskites, such as $CH_3NH_3PbI_3$ and $CH_3NH_3SnI_3$, have drawn intensive attention recently[1−7] because they can work as the light-absorber semiconducting materials in solar cells and have achieved high solar−electricity conversion efficiency over 15%.[8−10] As their inorganic counterpart, $CsSnI_3$ is also a semiconductor with a band gap around 1.3 eV,[11,12] thus potentially suitable for photovoltaic applications. However, the solar cells with $CsSnI_3$ as the light-absorber material (LAM) have thus far only achieved very low efficiency (0.2%[13] and 0.9%[14]), and the reason is not clear. One possible explanation is that $CsSnI_3$ has very high p-type electrical conductivity (EC), which makes the solar cells have low shunt resistance and, thus, low efficiency.[14] On the other hand, because of the high p-type EC and very high hole mobility (585 $cm^2\ V^{-1}\ s^{-1}$),[15] $CsSnI_3$ had also been considered as the hole-transport material (HTM) in solid-state dye-sensitized solar cells (DSSCs), with an energy-conversion efficiency of 3.7% [10.2% if the fluorine-doped $CsSn(I_{0.95},F_{0.05})_3$ is used].[13,16] In comparison to the conventional HTM in DSSCs, $CsSnI_3$ enhances the light absorption in red and near-infrared regions,[13] which indicates that it acts as not only HTM but also LAM, together with the wider band gap dyes.

Although $CsSnI_3$ had been used as both LAM and HTM experimentally,[13,14] which role it plays better in terms of performance (efficiency) is thus far not clear. The answer may depend upon how it is prepared and its material properties. For example, when the hole concentration and p-type EC are high, it works better as HTM, but when the hole concentration and p-type EC are moderate, it may work better as LAM. On the basis of this analysis, the hole-concentration control becomes necessary for optimizing the solar cell performance, regardless if $CsSnI_3$ is used as HTM or LAM. Because the carrier (hole or electron) concentration of semiconductors depends upon the concentration of intrinsic defects, a systematic study on the defect properties in $CsSnI_3$ becomes necessary.

The study on the defects is important for controlling not only the carrier concentration but also the recombination of the photogenerated electron−hole pairs, which is critical for LAM. Recently, it was found that strong photoluminescence (PL)[11] and high p-type EC, which are usually contradictive properties in normal semiconductors, can be combined in $CsSnI_3$.[15] This abnormal combination indicates that the $CsSnI_3$ sample has no

Received: August 25, 2014
Revised: September 20, 2014
Published: September 23, 2014

   dx.doi.org/10.1021/cm503122j | Chem. Mater. 2014, 26, 6068−6072

recombination-center defects when a high concentration of hole carriers and acceptor defects exists. To decrease EC and increase the shunt resistance, the formation of acceptor defects should be suppressed through changing the synthesis condition, but one question arises, i.e., whether recombination-center defects may form under the new condition? A study on a series of possible defects will be able to address this question.

Using first-principle calculations, here, we studied the formation and ionization of possible point defects in $CsSnI_3$ under different growth conditions. We found that (i) under a Sn-poor condition, the facile formation of the cation vacancy acceptor defects $V_{Cs}$ and $V_{Sn}$ contributes to the high p-type EC and all low-energy defects have resonant defect levels; thus, there is no recombination-center defect, which explains the abnormal combination of high EC and intense PL, and (ii) when Sn becomes richer, the concentration of acceptor defects decreases, whereas that of donor defects increases; therefore, the hole carrier concentration and, thus, the p-type EC decreases; meanwhile, the concentration of one deep-level defect, the $Sn_I$ antsisite, increases, which causes the non-radiative recombination of electron−hole pairs. On the basis of this, we predict that better performance can be achieved under a Sn-poor condition when $CsSnI_3$ is used as HTM, but a moderately Sn-rich (so that EC is not high) but not too rich (so that the concentration of $Sn_I$ is low) condition should be adopted when $CsSnI_3$ is used as LAM.

## 2. CALCULATION PROCEDURE AND METHODS

To predict what kind of defects will be formed in $CsSnI_3$, we calculated the formation energy of a series of possible intrinsic defects, including vacancies, antisites, and interstitials. For a defect $\alpha$ that is ionized to the charge state $q$, its formation energy $\Delta H^{\alpha,q}(\mu_i, E_F)$ is a function of the chemical potential of the component elements ($\mu_i$) and electrons ($E_F$, Fermi energy), which describes the richness of the elements or electrons in the synthesis environment[17−20]

$$\Delta H^{(\alpha,q)}(\mu_i, E_F) = \Delta H^{(\alpha,q)}(0, 0) + \sum_i n_i\mu_i + qE_F \quad (1)$$

where $\Delta H^{\alpha,q}(0, 0)$ is the formation energy when $\mu_i = 0$ and $E_F = 0$. $n_i(q)$ is the number of element $i$ (electron) removed from the host when forming the defect $\alpha$ in the charge state $q$, e.g., $n_{Cs} = -1$, $n_{Sn} = 1$, and $q = -1$ when forming $Cs_{Sn}^{1-}$ antisite defect (Cs replacing Sn, an acceptor that is ionized to −1 state). $E_F$ is referenced to the valence band maximum (VBM); therefore, $E_F = 0$ means that the Fermi energy is located at VBM. As the sample changes from heavily p type to heavily n type, $E_F$ shifts up from VBM to conduction band minimum (CBM). The chemical potential of elements is referenced to the pure elemental phases; therefore, $\mu_i = 0$ means that the element $i$ is so rich in the environment that its elemental phase can form; e.g., $\mu_{Sn} = 0$ means that Sn is so rich that the $\alpha$-Sn phase can form.

$\mu_{Cs}$, $\mu_{Sn}$, and $\mu_I$ are not free variables, and they are limited by a series of conditions to synthesize pure $CsSnI_3$. First, to avoid the leftover of (coexisting) Cs, Sn, or I elemental phases, it is required that $\mu_{Cs} < 0$, $\mu_{Sn} < 0$, $\mu_I < 0$. Second, to avoid the formation of the competing secondary compounds, such as CsI (orthorhombic structure, space group *Pnma*), the following condition must be satisfied too:

$$\mu_{Cs} + \mu_I < \Delta H_f(CsI) \quad (2)$$

where $\Delta H_f(CsI)$ is the formation energy of CsI referenced to stable bulk elements Cs and I. Similar conditions should also be satisfied to avoid other secondary compounds, $SnI_4$ (cubic structure, space group $Pa\bar{3}$), $SnI_2$ (monoclinic structure, space group $C2/m$),[21] and $Cs_2SnI_6$ (cubic structure, space group $Fm3m$).[22] Third, to make $CsSnI_3$ stable, the following thermodynamic equilibrium should be reached too:

$$\mu_{Cs} + \mu_{Sn} + 3\mu_I = \Delta H_f(CsSnI_3) \quad (3)$$

With all of these conditions satisfied, $\mu_{Cs}$ and $\mu_{Sn}$ (and, thus, $\mu_I$ determined according to eq 3) are limited in a narrow region, as shown by the blue region surrounded by A−B−C−D−E points in Figure 1. When the ($\mu_{Cs}$, $\mu_{Sn}$) point is on the right-hand side of the

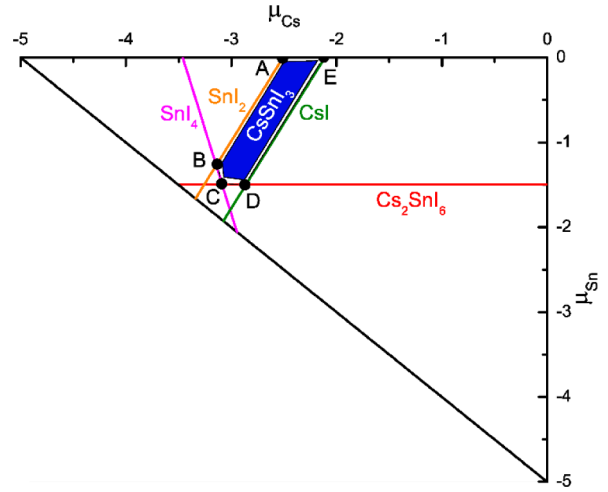


**Figure 1.** ($\mu_{Cs}$, $\mu_{Sn}$) chemical potential region (in blue) that stabilizes $CsSnI_3$ against other competitive phases, including Cs, Sn, I elemental phases and CsI, $SnI_2$, $SnI_4$, and $Cs_2SnI_6$ compounds.

D−E line, Cs is too rich in the environment and, thus, CsI will form, and when the ($\mu_{Cs}$, $\mu_{Sn}$) point is on the left-hand side of the A−B line, Cs is too poor and, thus, $SnI_2$ or $SnI_4$ will form. From the points A−E to B−C−D, Sn becomes poorer and poorer, and when the ($\mu_{Cs}$, $\mu_{Sn}$) point is below the C−D line, the Sn-poor phases $Cs_2SnI_6$ or CsI will form.

With the chemical potential region that stabilizes $CsSnI_3$ determined, now, we can calculate the formation energy of possible defects according to eq 1, in which the term $\Delta H^{\alpha,q}(0, 0)$ can be calculated using the supercell model (more details are given in refs 17−19 and 23). The total energy and band structure calculations are performed using the density functional theory methods as implemented in the Vienna *ab initio* simulation package (VASP) code.[24] The kinetic energy cutoff for the plane-wave basis is set to 300 eV. An 1 × 1 × 2 k-point mesh is used for the supercell with 80 atoms (the room-temperature black phase[15,25] of $CsSnI_3$ is studied here, with the lattice parameters and atomic coordinates listed in the Supporting Information). The Perdew−Burke−Ernzerhof (PBE)[26] exchange-correlation functional was employed. To correct the band gap underestimation in PBE calculation (the calculated value is only 0.52 eV with the spin−orbital coupling considered, significantly lower than the experimental value of 1.3 eV[11,12]), we have also performed self-consistent *GW* calculations.[27−29] The *GW* conduction (valence) band edge shifts up (down) by $\Delta_{CBM} = 0.21$ eV ($\Delta_{VBM} = 0.64$ eV) relative to the PBE one; therefore, the calculated band gap increases to 1.37 eV (with the spin−orbital coupling considered), in good agreement with the experimental value.[29] To correct the PBE error in the calculated formation energies of defects, we added the *GW* conduction (valence) band edge shift to the PBE formation energies of donor (acceptor) defects, because the PBE calculation underestmiates the formation energy by $\Delta_{CBM}$ per electron when there are electrons occupying the donor level ($\Delta_{VBM}$ per hole when there are holes occupying the acceptor level), as discussed in ref 30. For ionized defects, charged supercells are used and the electrostatic potential at atomic sites far from the defects is aligned for calculating the formation energy.[30] All of the calculated formation energies and trantion energy levels of defects in the present paper are after the *GW* band edge correction and with the spin−orbital coupling considered.


dx.doi.org/10.1021/cm503122j | *Chem. Mater.* 2014, 26, 6068−6072

## 3. FORMATION ENERGIES AND CONCENTRATION OF DEFECTS

The calculated formation energies are plotted in Figure 2 for a series of possible intrinsic defects, including $V_{Cs}$ (Cs vacancy),

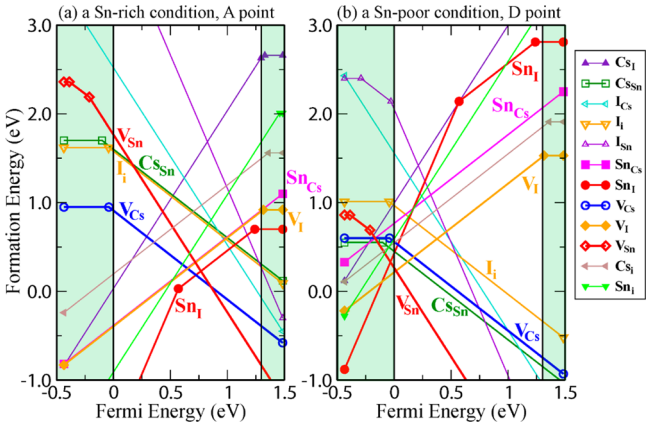


**Figure 2.** Calculated formation energy of defects as a function of the Fermi energy $E_F$ when ($\mu_{Cs}$, $\mu_{Sn}$) is at (a) A and (b) D points, as shown in Figure 1. The hollow and solid points denote acceptor and donor defects, respectively. According to eq 1, the slope of the function denotes the charge state $q$ of the defect and the Fermi energy at the turning point gives the transition energy level. The shaded regions with $E_F < 0$ eV and $E_F > 1.32$ eV show the valence band below VBM and the conduction band above CBM, respectively.

$V_{Sn}$, $V_I$, $Cs_{Sn}$ (Cs replacing Sn, antisite), $Sn_{Cs}$, $Cs_I$, $I_{Cs}$, $Sn_I$, $I_{Sn}$, $Cs_i$ (Cs interstitial), $Sn_i$, and $I_i$. Two chemical potential conditions are considered here, ($\mu_{Cs}$, $\mu_{Sn}$) at A (Sn-rich) and D (Sn-poor) points. Following eq 1, the formation energy of neutral defects does not change with the Fermi energy $E_F$, while that of ionized acceptor defects (such as $V_{Cs}^{-}$ and $V_{Sn}^{2-}$) decreases as $E_F$ increases (the slope is equal to the negative charge state $q$) and that of ionized donor defects (such as $Sn_I^{3+}$) increases as $E_F$ increases (the slope is equal to the positive charge state $q$).

Comparing the formation energies of different defects, we have the following observations: (i) Under the Sn-rich condition (Figure 2(a)), $V_{Cs}$ has the lowest formation energy among all acceptor defects, and $Sn_I$ has the lowest formation energy among all of the donor defects. However, both $V_{Cs}$ and $Sn_I$ have formation energies over 0.6 eV when the Fermi energy is at VBM and CBM, respectively; thus, their concentration is not high enough to pin the Fermi energy to either close to VBM or close to CBM. Their compensation (competition) will pin the Fermi energy at the middle of the band gap, 0.7 eV above VBM. Therefore, despite the concentrations of both $V_{Cs}$ and $Sn_I$ being high, the concentration of the hole carriers is low and, thus, the sample is intrinsic with a low EC under this Sn-rich condition. (ii) Under the Sn-poor condition (Figure 2(b)), $V_{Sn}$ becomes the dominant defect. The formation energy of ionized $V_{Sn}$ with $q = -2$ decreases to a negative value as $E_F$ shifts up to 0.2 eV above VBM; therefore, the Fermi energy is pinned to below this level, and the sample shows p-type conduction with a high hole concentration. Under this condition (Sn-poor; $E_F = 0.2$ eV), two ionized donor defects $V_I$ and $Sn_I$ have formation energies of 0.3 and 0.8 eV, respectively; therefore, a high concentration of $V_I$ may exist in the $CsSnI_3$ samples, but that of $Sn_I$ is much lower.

To show how the defect formation changes when the growth condition changes, in Figure 3, we plot the formation energy of

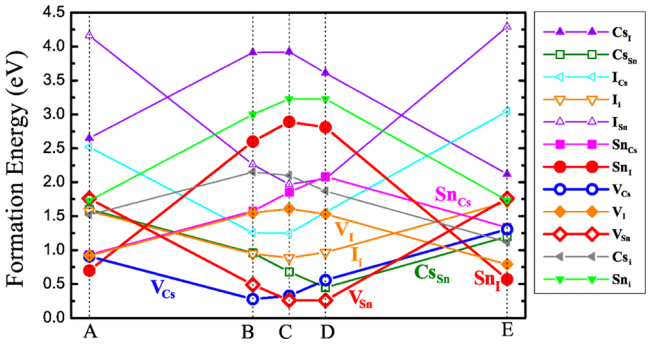


**Figure 3.** Calculated formation energy of defects as a function of the chemical potential, as ($\mu_{Cs}$, $\mu_{Sn}$) moves along the A−B−C−D−E line, as shown in Figure 1. The hollow and solid points denote acceptor and donor defects, respectively.

different defects as a function of the chemical potential ($\mu_{Cs}$, $\mu_{Sn}$). For acceptor defects, their formation energies at $E_F = 0$ eV (VBM) are plotted, while for donor defects, their formation energies at $E_F = 1.32$ eV (CBM) are plotted. When the plotted formation energy of acceptor defects are significantly lower than that of the donor defects, the higher concentration of acceptor defects will pin Fermi energy close to VBM and, thus, the sample will be p-type, which is the case at B, C, and D points (shown in both Figures 2 and 3, $V_{Cs}$ and $V_{Sn}$ have much lower energy than all donor defects). In contrast, when the formation energies of the acceptor and donor defects are comparable (the difference is not large), the competition between them will pin the Fermi energy at the middle of the band gap and the samples will have a low EC, which is the case at A and E points.

As seen in Figure 3, the lowest formation energy of acceptor defects increases, while that of donor defects decreases as ($\mu_{Cs}$, $\mu_{Sn}$) moves from B−C−D points to A−E points, i.e., from Sn-poor conditions to Sn-rich conditions. This indicates that the hole carrier concentration and, thus, the p-type EC will decrease as Sn becomes richer in the growth environment and Sn richness can be used to control the EC of $CsSnI_3$ samples. Because the sample is intrinsic with a low EC under the Sn-rich condition, we can predict that the experimentally observed high p-type EC[14,15] should be in Sn-poor samples, in which a high concentration of hole carriers can be generated by $V_{Cs}$ or $V_{Sn}$ acceptor defects with very low formation energy (as low as 0.25 eV) and, thus, very high concentration (as high as $10^{19}$ $cm^{-3}$). Experimentally, the Sn deficiency had also been found in $CsSnI_3$ samples by X-ray fluorescence (XRF).[11] On the other hand, our calculations also show that the highest achievable Fermi energy under the richest Sn condition is limited to lower than 0.45 eV below CBM; therefore, the highest electron concentration in $CsSnI_3$ is also limited; i.e., a poor n-type EC may be possible under a Sn-rich condition, consistent with the experimental observation of a low electron carrier concentration at $10^7$ $cm^{-3}$ by Stoumpos et al.,[31] but a high n-type EC is difficult to achieve in $CsSnI_3$. We noticed that a previous calculation[15] had predicted negative formation energies of $V_{Sn}$ and $V_{Cs}$ acceptor defects under both Sn-rich and Sn-poor conditions, which means that these defects and hole carriers will always have an extremely high concentration in $CsSnI_3$ samples. This prediction is inconsistent with our current study


dx.doi.org/10.1021/cm503122j | Chem. Mater. 2014, 26, 6068−6072

and the experimental observation that the hole carrier density[15] is in the order of $10^{17}$ $cm^{-3}$, and the sample can be even n-type.[31] Our test calculations showed that this inconsistency may result from the band gap underestimation associated with the local density approximation (LDA) adopted in the previous study.[15] Negative formation energies had also been found if we did not include the spin−orbital coupling in the band gap calculation and did not perform *GW* calculation to correct the band gap underestimation.

## 4. DEFECT ENERGY LEVELS AND THEIR INFLUENCE ON PHOTOVOTAIC PERFORMANCE

Above, we discussed the formation and concentration of defects; however, whether these defects contribute to the carrier concentration and EC depends upon their ionization, which is determined by their transition energy levels. The transition energy level $\varepsilon_\alpha(q/q')$ is defined as the Fermi energy at which the defects $\alpha$ with two different charge states $q$ and $q'$ have the same formation energy;[17] therefore, the defects can release electrons or holes and change their charge state from $q$ to $q'$ or vice versa at $\varepsilon_\alpha(q/q')$. They are located at the turning points in the formation energy plot as a function of the Fermi energy, as shown in Figure 2. For example, the turning point of $V_{Cs}$ from the neutral charge state ($q = 0$) to the ionized state ($q = -1$) is located at $E_F = -0.04$ eV; thus, its ($-/0$) transition energy level is located at 0.04 eV below VBM.

In Figure 4, the calculated transition energy levels of various defects between different charge states are plotted relative to

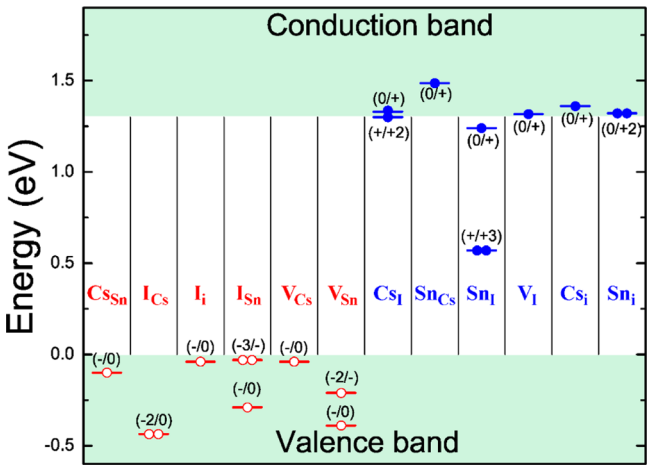


**Figure 4.** Calculated transition energy levels for various intrinsic defects. The regions under VBM and above CBM are in shaded color. Acceptor and donor defect levels are denoted by red and blue lines, respectively. The hollow (solid) points at the levels show the number of hole (electron) carriers that can be released during the transition of the defect charge state.

the valence and conduction band edges. Interestingly, the transition energy levels of all of the acceptor defects are resonant in the valence band (located below VBM), which means that they are all ionized once formed. The low ionization energy of the acceptor defect relative to VBM is caused by the high p orbital energy of I and the strong hybridization between the Sn 5s and I 5p states, whose anti-bonding state composes the VBM of $CsSnI_3$.[29] Each ionized $V_{Cs}$ ($q = -1$) generates one hole carrier, and each ionized $V_{Sn}$ ($q = -2$) generates two hole carriers; therefore, a high concentration of $V_{Cs}$ and $V_{Sn}$ lead to a high concentration of hole carriers and, thus, high EC, supporting our above discussion.

On the donor-defect side, most of them have resonant donor levels inside the conduction bands, such as $Cs_i$, $Cs_I$, $V_I$, etc. The sole exception is the $Sn_I$ antisite. Because of the low local symmetry at the I site, Sn 5p orbitals split, creating a shallow (0/+) level near the CBM but also a deep (+1/+3) level at the middle of the band gap. Under the Sn-rich condition, this deep-level defect can have a high concentration, which is in contrast with the case in the organometal halide $CH_3NH_3PbI_3$, where all of the dominant defects create only shallow levels under both the Pb-rich or Pb-poor conditions.[32] We noticed that, in a previous study,[15] $Sn_I$ was taken as an acceptor defect; however, our current calculations showed clearly that it produces occupied defect levels closer to the CBM; therefore, it is characterized as a donor and not an acceptor. In p-type $CsSnI_3$, the $Sn_I$ defect will act as an electron trap and recombination center of the photogenerated electron−hole pairs; thus, a high concentration of $Sn_I$ is detrimental to the solar cell performance if $CsSnI_3$ is used as LAM. On the basis of this, a Sn-poor condition should be used to suppress the $Sn_I$ concentration in the synthesized $CsSnI_3$ samples. However, a too Sn-poor condition will cause too high hole concentration and EC and, thus, low shunt resistance, which is also detrimental to the solar cell performance. The trade-off between the two factors requires that a moderate Sn chemical potential (neither too rich nor too poor) should be used to synthesize $CsSnI_3$ as LAM.

On the basis of the above calculated results and discussions on how the defects influence EC and electron−hole recombination, we can now explain why the high EC and strong PL can be combined in $CsSnI_3$. Obviously, under the Sn-rich condition, the EC is low due to strong defect compensation and a high concentration of $Sn_I$ defects can cause non-radiative recombination of electron−hole pairs; therefore, the carrier lifetime will be low. However, under the Sn-poor condition, a high concentration of acceptor defects generate a high concentration of hole carriers and all defects with a high concentration are not recombination centers; therefore, the abnormal combination of high EC and strong PL becomes possible. Because all high-concentration defects have resonant defect levels, as shown in Figure 4, the strong PL should result from the transition between the conduction and valence band edges. Experimentally, a PL peak at 950 nm (1.31 eV in energy, close to the experimental band gap) was observed,[12,15] which agrees well with our predicted transitions between the band edges. This abnormal combination is good for the solar cell performance when $CsSnI_3$ is used as HTM, because a high p-type EC enhances the hole transport, and meanwhile, the disappearance of recombination centers (strong PL) increases the carrier lifetime and hole-diffusion length. Therefore, a Sn-poor condition should be used to synthesize $CsSnI_3$ as HTM.

## 5. CONCLUSION

In conclusion, the defects and their influence on the carrier generation and recombination in $CsSnI_3$ are studied using the first-principle calculations. Under the Sn-poor growth condition, we found that a high concentration of ionized $V_{Cs}$ and $V_{Sn}$ acceptor defects can form and generate a high concentration of hole carriers and there is no low-energy defects acting as recombination centers; therefore, high EC and strong PL can coexist in $CsSnI_3$. As Sn becomes richer, the


dx.doi.org/10.1021/cm503122j | *Chem. Mater.* 2014, 26, 6068−6072

concentration of acceptor defects decreases, while that of donor defects, such as $Sn_I$ and $V_I$, increases; therefore, the EC changes from highly p type to intrinsic and to even weakly n type. $Sn_I$ is the only intrinsic defect that produces a deep donor level in the band gap and acts as an electron−hole recombination center. On the basis of this, we suggest that a Sn-poor condition should be used to synthesize highly p-type conductive $CsSnI_3$ as HTM; however, when $CsSnI_3$ is used as LAM, a moderately Sn-rich condition should be used to control the concentration of hole carriers (thus EC) to a moderate level and suppress the $Sn_I$ antisite concentration to a low level. These results provide atomic-level insights for optimizing $CsSnI_3$ and related organometal halide solar cell performance. Experimental identification of these low-energy defects is needed.

## ■ ASSOCIATED CONTENT

### Supporting Information

Lattice constants (in angstroms) and atomic coordinates (relative to the basis vectors) of the orthorhombic $CsSnI_3$ (room-temperature black phase) (Table S1). This material is available free of charge via the Internet at http://pubs.acs.org.

## ■ AUTHOR INFORMATION


### Corresponding Authors

*E-mail: (S.C.) chensy@ee.ecnu.edu.cn.
*E-mail: (X.-G.G.) xggong@fudan.edu.cn.
*E-mail: (S.-H.W.) suhuai.wei@nrel.gov.


### Notes

The authors declare no competing financial interest.

## ■ ACKNOWLEDGMENTS

The work at Fudan University was supported by the Special Funds for Major State Basic Research, the National Natural Science Foundation of China (NSFC), the International Collaboration Project, and the Program for Professor of Special Appointment (Eastern Scholar). Shiyou Chen is supported by the NSFC under Grants 61106087, 91233121, and 10934002 and the Shanghai Rising-Star Program (14QA1401500). The work at NREL was funded by the United States Department of Energy (U.S. DOE) under Contract DE-AC36-08GO28308.

## ■ REFERENCES


(1) Xing, G.; Mathews, N.; Sun, S.; Lim, S. S.; Lam, Y. M.; Gratzel, M.; Mhaisalkar, S.; Sum, T. C. *Science* **2013**, *342*, 344.
(2) Stranks, S. D.; Eperon, G. E.; Grancini, G.; Menelaou, C.; Alcocer, M. J.; Leijtens, T.; Herz, L. M.; Petrozza, A.; Snaith, H. J. *Science* **2013**, *342*, 341.
(3) Lee, M. M.; Teuscher, J.; Miyasaka, T.; Murakami, T. N.; Snaith, H. J. *Science* **2012**, *338*, 643.
(4) Frost, J. M.; Butler, K. T.; Brivio, F.; Hendon, C. H.; van Schilfgaarde, M.; Walsh, A. *Nano Lett.* **2014**, *14*, 2584.
(5) Yin, W.-J.; Shi, T.; Yan, Y. *Adv. Mater.* **2014**, *26*, 4653.
(6) Du, M. H. *J. Mater. Chem. A* **2014**, *2*, 9091.
(7) Chiarella, F.; Zappettini, A.; Licci, F.; Borriello, I.; Cantele, G.; Ninno, D.; Cassinese, A.; Vaglio, R. *Phys. Rev. B: Condens. Matter Mater. Phys.* **2008**, *77*, 045129.
(8) Liu, M.; Johnston, M. B.; Snaith, H. J. *Nature* **2013**, *501*, 395.
(9) Burschka, J.; Pellet, N.; Moon, S. J.; Humphry-Baker, R.; Gao, P.; Nazeeruddin, M. K.; Gratzel, M. *Nature* **2013**, *499*, 316.
(10) Zhou, H.; Chen, Q.; Li, G.; Luo, S.; Song, T.-b.; Duan, H.-S.; Hong, Z.; You, J.; Liu, Y.; Yang, Y. *Science* **2014**, *345*, 542.
(11) Shum, K.; Chen, Z.; Qureshi, J.; Yu, C.; Wang, J. J.; Pfenninger, W.; Vockic, N.; Midgley, J.; Kenney, J. T. *Appl. Phys. Lett.* **2010**, *96*, 221903.
(12) Chen, Z.; Yu, C.; Shum, K.; Wang, J. J.; Pfenninger, W.; Vockic, N.; Midgley, J.; Kenney, J. T. *J. Lumin.* **2012**, *132*, 345.
(13) Chung, I.; Lee, B.; He, J.; Chang, R. P.; Kanatzidis, M. G. *Nature* **2012**, *485*, 486.
(14) Chen, Z.; Wang, J. J.; Ren, Y.; Yu, C.; Shum, K. *Appl. Phys. Lett.* **2012**, *101*, 093901.
(15) Chung, I.; Song, J. H.; Im, J.; Androulakis, J.; Malliakas, C. D.; Li, H.; Freeman, A. J.; Kenney, J. T.; Kanatzidis, M. G. *J. Am. Chem. Soc.* **2012**, *134*, 8579.
(16) Zhang, Q.; Liu, X. *Small* **2012**, *8*, 3711.
(17) Wei, S.-H. *Comput. Mater. Sci.* **2004**, *30*, 337.
(18) Wei, S.-H.; Zhang, S. *Phys. Rev. B: Condens. Matter Mater. Phys.* **2002**, *66*, 155211.
(19) Chen, S.; Walsh, A.; Gong, X. G.; Wei, S. H. *Adv. Mater.* **2013**, *25*, 1522.
(20) Yang, J.-H.; Chen, S.; Xiang, H.; Gong, X. G.; Wei, S.-H. *Phys. Rev. B: Condens. Matter Mater. Phys.* **2011**, *83*, 235208.
(21) Howie, R. A.; Moser, W.; Trevena, I. C. *Acta Crystallogr., Sect. B: Struct. Crystallogr. Cryst. Chem.* **1972**, *28*, 2965.
(22) Tudela, D.; Sanchez-Herencia, A. J.; Diaz, M.; Fernandez-Ruiz, R.; Menendez, N.; Tornero, J. D. *Dalton Trans.* **1999**, *1999*, 4019.
(23) Chen, S.; Yang, J.-H.; Gong, X. G.; Walsh, A.; Wei, S.-H. *Phys. Rev. B: Condens. Matter Mater. Phys.* **2010**, *81*, 245204.
(24) Kresse, G.; Furthmuller, J. *Phys. Rev. B: Condens. Matter Mater. Phys.* **1996**, *54*, 11169.
(25) Yamada, K.; Funabiki, S.; Horimoto, H.; Matsui, T.; Okuda, T.; Ichiba, S. *Chem. Lett.* **1991**, *20*, 801.
(26) Perdew, J. P.; Burke, K.; Ernzerhof, M. *Phys. Rev. Lett.* **1996**, *77*, 3865.
(27) Shishkin, M.; Kresse, G. *Phys. Rev. B: Condens. Matter Mater. Phys.* **2007**, *75*, 235102.
(28) Brivio, F.; Butler, K. T.; Walsh, A.; van Schilfgaarde, M. *Phys. Rev. B: Condens. Matter Mater. Phys.* **2014**, *89*, 155204.
(29) Huang, L. Y.; Lambrecht, W. R. L. *Phys. Rev. B: Condens. Matter Mater. Phys.* **2013**, *88*, 165203.
(30) Lany, S.; Zunger, A. *Phys. Rev. B: Condens. Matter Mater. Phys.* **2008**, *78*, 235104.
(31) Stoumpos, C. C.; Malliakas, C. D.; Kanatzidis, M. G. *Inorg. Chem.* **2013**, *52*, 9019.
(32) Yin, W.-J.; Shi, T.; Yan, Y. *Appl. Phys. Lett.* **2014**, *104*, 063903.